JOURNAL OF SPACECRAFT AND ROCKETS
Vol. 42, No. 5, September–October 2005

Improved Method of Mixed-Boundary Component-Mode Representation for Structural Dynamic Analysis

A. Majed* and E. E. Henkel†
Applied Structural Dynamics, Inc., Houston, Texas 77277
and
C. Wilson‡
MSC Software Corporation, Los Angeles, California 90041

An improved method of mixed-boundary component representation is presented. This residual flexibility mixed-boundary (RFMB) method presents two compelling features over the existing mixed-boundary methods. First, RFMB is accurate for the entire range of component boundary representations, that is, from all-fixed to mixed to all-free boundaries; therefore, resorting to other methods to cover the all-fixed- or all-free-boundary cases is not necessary. Second, all parameters for the RFMB generalized stiffness matrix can be directly derived from component test, resulting in a more rigorous definition of test/analysis correlation. Two example problems are presented, demonstrating the benefits of the subject method. This new RFMB method has been implemented in the latest release of the general purpose finite element program, MSC.Nastran, as the default.

Nomenclature

$\bar{B}$	=	fixed-boundary physical coordinate set
$\bar{C}$	=	free-boundary physical coordinate set
c	=	damping matrix
g	=	flexibility matrix
I	=	identity matrix
$\bar{I}$	=	interior physical coordinate set
i	=	imaginary number, $\sqrt{-1}$
k	=	stiffness matrix
m	=	mass matrix
$\bar{P}$	=	physical coordinate set
q	=	generalized coordinates
T	=	transformation matrix
$\bar{T}$	=	total boundary physical coordinate set
x	=	physical degrees of freedom
ζ	=	modal damping coefficient
κ	=	generalized stiffness matrix
μ	=	generalized mass matrix
ϕ	=	normal modes
ψ	=	constraint modes
ω	=	modal frequencies
ϖ	=	frequency parameter

Subscripts

b, c, i, p, r, t	=	number of degrees of freedom in various physical coordinate sets
k	=	number of kept normal modes

Superscripts

C	=	constraint modes
I	=	inertia-relief modes
N	=	normal modes
R	=	residual contribution
T	=	total flexibility contribution
$()'$	=	transpose of a matrix

Received 16 February 2004; revision received 17 August 2004; accepted for publication 30 August 2004.

*Chief, Structural Dynamics/Advanced Methods. Senior Member AIAA.
†Chief Engineer. Senior Member AIAA.
‡Manager, MSC.Nastran Methods, 815 Colorado Boulevard.

I. Introduction

COMPONENT-MODE synthesis (CMS) is a highly efficient means of substructure coupling for dynamic analysis, in which each component is represented by a linear superposition of its component modes rather than a large number of physical coordinates. In his latest survey paper, Craig[1] gives an excellent overview of CMS methods including the fixed-boundary methods of Hurty[2] and Craig and Bampton,[3] the free-boundary methods of MacNeal[4] and Rubin,[5] the boundary-loaded method of Benfield and Hruda,[6] and the mixed-boundary method of Hintz.[7] (Component modes determined by boundary loading are modified to more closely resemble system modes that will improve the accuracy of system results.)

Studies such as that by Collins et al.[8] on the fixed-boundary method of Hurty and its derivative (e.g., the equivalent method of Craig and Bampton, henceforth referred to as Hurty/Craig–Bampton in this paper) have led to the conclusion that fixed-boundary methods tend to converge best when there are not a large number of boundary coordinates involved. The reason for this is that fixed-boundary methods require the normal modes to be computed relative to the entire set of boundary coordinates, leading to overconstrained normal modes. Because it is a likely scenario that the component boundary conditions in the coupled system are a subset of the overall component boundary coordinates, the issue of proper truncation of these overconstrained normal modes for adequate convergence naturally arises.

Mixed-boundary component-mode representation allows the analyst the freedom to employ normal modes with a mixture of fixed and free boundaries. The ability to use component normal modes with any boundary conditions results in a more accurate component representation with a minimum number of degrees of freedom (DOF), that is, because the boundary conditions on the component normal modes can be the same as the component in the coupled system, modal convergence is significantly enhanced. This also leads to a simple criterion for the component frequency truncation. Therefore, component convergence issues associated with all-fixed- and all-free-boundary methods are mitigated. In addition, because the boundary conditions on the normal modes can be the same as the component modal test, a simpler definition of the component damping matrix results.

Table 1 Desired characteristics for a mixed-boundary method

Desired characteristics for a mixed-boundary method	HMB	MHMB	RFMB	RFMB-V
1) Accurate for all component boundary conditions	×	×	√	√
2) Explicit inclusion of boundary physical coordinates	×	√	√	√
3) Component independence	√	√	√	√
4) Statically complete	√	√	√	√
5) Test compatibility	×	×	√	×

It is highly desirable for a mixed-boundary method to possess the following characteristics:

1) Accuracy is the first characteristic. The method should yield an accurate representation of the component dynamics for all component boundary conditions including all fixed and all free. The robust and time-tested methods of Hurty/Craig–Bampton (for all-fixed boundary) and Rubin (for all-free boundary) will be used to measure the accuracy of the various mixed-boundary methods for the all-fixed- and all-free-boundary cases.

2) Explicit inclusion of physical boundary coordinates is the second characteristic. The method should conform to simple direct stiffness CMS (component coupling) and not require any special coupling procedures.

3) The third characteristic is component independence. The method should be independent of other components' stiffness and mass boundary data.

4) The fourth characteristic is that the method should be statically complete. The method should give the exact static solution for the component.

5) The final characteristic is test compatibility. The method's stiffness representation should be directly derivable from the component test, that is, test/analysis correlation for all individual parameters comprising the component generalized stiffness matrix should be possible.

The mixed-boundary approach was first developed by Hintz.[7] In his paper, Hintz presented two equivalent generalized methods to component reduction. Hintz's method of constraint modes involves a superposition of four component mode sets: 1) rigid-body modes, 2) redundant boundary constraint modes, 3) inertia-relief modes, which are static displacements caused by rigid-body accelerations, and 4) normal modes with any boundary condition. Hintz's method of attachment modes replaces the constraint mode set with an attachment mode set. Because attachment modes and constraint modes span the same space, the methods are equivalent. Because the resulting component boundary coordinates are expressed in generalized coordinates, Hintz's mixed-boundary (HMB) method, as presented in Ref. 7, requires a special coupling procedure. Hintz demonstrates the convergence characteristics of his method by solving the classic CMS benchmark problem, the Benfield truss (also used in this paper). The results demonstrate that, for the same number of DOF retained in the coupled system, the presence of inertia-relief modes in the HMB method results in superior convergence (relative to Hurty/Craig–Bampton method) for the lower-frequency modes, whereas the opposite is true for the higher frequencies (discussed in Sec. III). The HMB method leads to generalized stiffness parameters that cannot be directly determined from component test. Therefore, the HMB method does not meet characteristics 1, 2, and 5. (Note: the need for a special coupling procedure for HMB method can be mitigated with some additional mathematics; this results in a HMB coordinate transformation with explicit inclusion of boundary DOF, given in this paper).

A variation of Hintz's method of constraint modes is typically used in general-purpose finite element programs such as MSC.Nastran for mixed-boundary CMS. The method does not make a distinction between statically determinate and redundant boundary coordinates in the calculation of the constraint modes. The method employs constraint modes for the fixed-boundary and free-boundary coordinates, supplemented with normal modes relative to the fixed-boundary coordinates. Unlike the HMB method, the method does not use inertia-relief modes; thereby avoiding the increased potential for rank-deficiency (discussed in Sec. V). This modified-Hintz mixed-boundary (MHMB) method does provide physical coordinates for standard CMS component coupling and is exactly equal to the Hurty/Craig–Bampton method for the all-fixed-boundary case. However, it demonstrates weak convergence for the all-free-boundary case. As is the case with the HMB method, it will be demonstrated that the MHMB method generalized stiffness cannot be directly determined from component test. Therefore, the MHMB method does not meet characteristics 1 and 5.

The residual flexibility mixed-boundary (RFMB) method described in this paper provides an improved means of conducting mixed-boundary component reductions. The method utilizes three mutually linearly independent mode sets. Two of the mode sets, residual flexibility modes (representing the free-boundary coupling) and a truncated set of normal modes (relative to the fixed boundary), are mutually orthogonal relative to stiffness and mass. The third mode set, the constraint modes (representing the fixed-boundary coupling), is linearly independent to the other mode sets by the virtue of the boundary conditions. Most notably, it will be demonstrated that all parameters in the RFMB generalized stiffness can be directly derived from component test.

It is useful to think of the RFMB method as an expansion of the Hurty/Craig–Bampton method, where additional free-boundary physical coordinates are added via residual flexibility. In this way, the boundary conditions on the normal modes are not affected, as would be the case in the Hurty/Craig–Bampton or other fixed-boundary approaches. The resulting RFMB coordinate transformation is exactly equal to the accurate and time-tested methods of Hurty/Craig–Bampton and Rubin for the bounding cases of all-fixed boundary and all-free boundary, respectively. Therefore, the method is accurate for the entire spectrum of component representation, from all-fixed to mixed to all-free boundary. The method meets all desired characteristics of a mixed-boundary method given in Table 1. Note that Table 1 also mentions RFMB-V, an equivalent variant to RFMB involving total flexibility that will be discussed later in the paper.

An example problem using the classical Benfield-truss CMS problem is exercised to demonstrate the RFMB method's convergence for the cases of all-fixed and all-free boundaries. The results are compared to that of MHMB method. A second example involving a Space Shuttle Orbiter cargo carrier is presented, comparing the convergence of the RFMB method vs Hurty/Craig–Bampton.

II. Residual Flexibility Mixed-Boundary Method

A. Definitions: Coordinate Sets and Component Modes

Let the unreduced component stiffness and mass matrices be denoted by k and m, respectively. The total set of physical coordinates is denoted by $\bar{P}$. These coordinate sets contain p, i, and t DOF, respectively. For the purposes of mixed boundary, let the $\bar{T}$ set be composed of the union of the $\bar{B}$ and $\bar{C}$ sets, where the $\bar{B}$ set is fixed in the normal modes problem, while the $\bar{C}$ set is free to participate in the normal modes. These sets contain b and c DOF, respectively.

The subject mixed-boundary method uses three component mode sets: constraint modes caused by unit displacement application on the $\bar{B}$ set, residual flexibility modes caused by unit force application on the $\bar{C}$ set (with the kept modal flexibility removed), and a truncated set of normal modes with the $\bar{B}$ set fixed. The derivation of these component mode sets is given in Craig's latest CMS survey paper.[1] Other references in which constraint modes are discussed include Refs. 2, 3, and 7. Residual flexibility was first introduced by MacNeal[4] and is also derived in Rubin's paper[5] for an all-free-boundary case. As is the case in the Hurty/Craig–Bampton method, the $\bar{B}$ set is at a minimum sufficient to restrain the component from rigid-body motion. For the all-free-boundary case, that is, all boundary coordinates in the $\bar{C}$ set, the residual flexibility calculation involves inertia relief as in Rubin's method.

The constraint mode set is denoted by ψ_b^C, containing b vectors with the superscript C denoting constraint modes. The residual flexibility mode set is denoted by g_c^R, containing c vectors. The truncated normal mode set is denoted by ϕ_k^N, containing k normal modes.

B. Derivation of the Coordinate Transformation

Using the Rayleigh–Ritz approach, the component physical coordinate x can be written as a linear superposition of the three component mode sets as

$$x = \psi_b^C q^C + g_c^R q^R + \phi_k^N q^N \tag{1}$$

where the generalized coordinate related to each mode set is denoted by q. Equation (1) can be partitioned into three equations as follows:

$$x_b = q^C \tag{2a}$$

$$x_c = \psi_{\text{cb}}^C q^C + g_{\text{cc}}^R q^R + \phi_{\text{ck}}^N q^N \tag{2b}$$

$$x_i = \psi_{\text{ib}}^C q^C + g_{\text{ic}}^R q^R + \phi_{\text{ic}}^N q^N \tag{2c}$$

or simply,

$$x = T_1 q_1 \tag{3}$$

where $q_1 = \lfloor x_b \;\; q^R \;\; q^N \rfloor'$ denotes the component's generalized coordinate space. It is apparent from the constraint modes that Eq. (2a) provides physical coordinates for the $\bar{B}$ set; however, Eqs. (2b) and (2c) do not provide physical coordinates for the $\bar{C}$ set. This issue can be resolved because g_{cc}^R is nonsingular (further addressed in Sec. II.E), allowing the solution of the residual generalized coordinates in terms of the $\bar{C}$ set, resulting in

$$x_b = x_b \tag{4a}$$

$$q^R = -g_{\text{cc}}^{R^{-1}} \left(\psi_{\text{cb}}^C x_b - x_c + \phi_{\text{ck}}^N q^N \right) \tag{4b}$$

$$q^N = q^N \tag{4c}$$

or simply,

$$q_1 = T_2 q_2 \tag{5}$$

where $q_2 = \lfloor x_b \;\; x_c \;\; q_k \rfloor'$ denotes the component's mixed-boundary coordinate space. (Note: the subscript k denotes a truncated set of k normal modes.) Therefore, the subject method's coordinate transformation from the component physical coordinates to the mixed-boundary coordinates can be written as

$$x = T_1 T_2 q_2 \tag{6}$$

or

$$\begin{Bmatrix} x_b \\ x_c \\ x_i \end{Bmatrix} = \begin{bmatrix} \backslash I_{b\backslash} & 0 & 0 \\ 0 & \backslash I_{c\backslash} & 0 \\ \psi_{\text{ib}}^C - g_{\text{ic}}^R g_{\text{cc}}^{R^{-1}} \psi_{\text{cb}}^C & g_{\text{ic}}^R g_{\text{cc}}^{R^{-1}} & \phi_{\text{ik}}^N - g_{\text{ic}}^R g_{\text{cc}}^{R^{-1}} \phi_{\text{ck}}^N \end{bmatrix} \begin{Bmatrix} x_b \\ x_c \\ q_k \end{Bmatrix} \tag{7}$$

In physical terms, the $\bar{B}$ and $\bar{C}$ set DOF are statically complete. The static contribution to the $\bar{I}$ set displacements from the $\bar{B}$ set displacements is in the 3-1 partition. Because the $\bar{C}$ set DOF participate in the static displacements as a result of $\bar{B}$ set displacements, the residual contribution to the $\bar{I}$ set DOF from this is subtracted out of the 3-1 partition term. The $\bar{C}$ set residual contribution to $\bar{I}$ set is totally accounted for in the 3-2 partition term.

1. All-Fixed-Boundary Case: Exact Reduction to the Hurty/Craig–Bampton Method

The RFMB coordinate transformation exactly reduces to the method of Hurty/Craig–Bampton for the all-fixed-boundary case, that is, no $\bar{C}$ set DOF.

$$\begin{Bmatrix} x_b \\ x_i \end{Bmatrix} = \begin{bmatrix} \backslash I_{b\backslash} & 0 \\ \psi_{\text{ib}}^C & \phi_{\text{ik}}^N \end{bmatrix} \begin{Bmatrix} x_b \\ q_k \end{Bmatrix} \tag{8}$$

2. All-Free-Boundary Case: Exact Reduction to Rubin's Method

The RFMB coordinate transformation exactly reduces to the method of Rubin for the all-free-boundary case, that is, no $\bar{B}$ set DOF.

$$\begin{Bmatrix} x_c \\ x_i \end{Bmatrix} = \begin{bmatrix} \backslash I_{c\backslash} & 0 \\ g_{\text{ic}}^R g_{\text{cc}}^{R^{-1}} & \phi_{\text{ik}}^N - g_{\text{ic}}^R g_{\text{cc}}^{R^{-1}} \phi_{\text{ck}}^N \end{bmatrix} \begin{Bmatrix} x_c \\ q_k \end{Bmatrix} \tag{9}$$

Therefore, the RFMB transformation of Eq. (7) is a generalization of the robust and widely used methods of Hurty/Craig–Bampton and Rubin.

C. Component Stiffness and Mass Matrices

Because the RFMB method utilizes mutually linearly independent mode sets, the resulting generalized stiffness matrix (in the $q_1 = \lfloor x_b \;\; q^R \;\; q^N \rfloor'$ space) is given by

$$\kappa_1^{\text{RFMB}} = T_1' k T_1 = \begin{bmatrix} \kappa_{\text{bb}} & & \\ & g_{\text{cc}}^R & \\ & & \backslash \omega_{k\backslash}^2 \end{bmatrix} \tag{10}$$

where κ_{bb} is the $\bar{B}$ set Guyan reduced stiffness matrix (same as utilized in the Hurty/Craig–Bampton method), g_{cc}^R is the $\bar{C}$ set residual flexibility matrix, and ω_k^2 are the component eigenvalues relative to the $\bar{B}$ set DOF. (Eigenvectors are normalized to identity mass throughout this paper.) Note that there are no cross-coupling terms.

The component generalized mass matrix is given by

$$\mu_1^{\text{RFMB}} = T_1' m T_1 = \begin{bmatrix} \mu_{\text{bb}} & \mu_{\text{bc}}^R & \mu_{\text{bk}} \\ \mu_{\text{cb}}^R & \mu_{\text{cc}}^R & 0 \\ \mu_{\text{kb}} & 0 & \backslash I_{k\backslash} \end{bmatrix} \tag{11}$$

where μ_{bb} is the $\bar{B}$ set Guyan reduced mass matrix (again, the same as used in the Hurty/Craig–Bampton method), μ_{bk} is the $\bar{B}$ set mass coupling terms to the normal modes (the same as in the Hurty/Craig–Bampton method), and μ_{cc}^R is Rubin's residual mass. The additional mass coupling term, not present in the Hurty/Craig–Bampton and Rubin's methods, is given by

$$\mu_{\text{cb}}^R = \mu_{\text{bc}}^{R'} = g_c^{R'} m \psi_b^C \tag{12}$$

which represents the mass coupling terms between the $\bar{B}$ and $\bar{C}$ sets.

The mixed-boundary stiffness and mass matrices in the q_2 (mixed-boundary) coordinates are then given by the following equations:

$$\kappa_2 = T_2' \kappa_1 T_2 \tag{13}$$

$$\mu_2 = T_2' \mu_1 T_2 \tag{14}$$

It goes without saying that a direct triple product of the RFMB coordinate transformation, Eq. (7), with the component stiffness and mass matrices will result in the same mixed-boundary stiffness and mass matrices as in Eqs. (13) and (14). The generalized stiffness and mass matrices derived in Eqs. (10) and (11) are equivalent to the mixed-boundary stiffness and mass given in Eqs. (13) and (14). Equations (10) and (11) are derived for subsequent use in Sec. IV of the paper.

D. Component Damping Matrix

Because the component mixed-boundary reduction can employ normal modes with any boundary conditions without regard to the $\bar{C}$ set physical coordinates, it might be useful to use boundary conditions that replicate the component modal test configuration. With this, the damping matrix is simply defined as follows:

$$c_2 = \begin{bmatrix} 0 & & \\ & 0 & \\ & & \backslash 2\zeta\omega \backslash \end{bmatrix} \tag{15}$$

where ζ is the modal damping ratio measured for each component normal mode. Because the $\bar{C}$ set physical DOF "participate" in the normal modes, they are inherently damped, that is, a forced input into a $\bar{C}$ set physical DOF will necessarily drive the normal modal coordinates, which are damped via Eq. (15). It is recognized that the contribution from Rubin's residual damping term c_{cc}^R is not included in Eq. (15).

III. Mixed-Boundary Variants

The HMB component boundary mode set involves rigid-body modes, redundant boundary constraint modes, and inertia-relief modes. Inertia-relief modes are static displacements caused by imposed rigid-body accelerations with the component supported such that the stiffness matrix is not singular. This statically complete boundary mode set is then supplemented with normal modes with any boundary conditions. Though HMB as originally derived in Ref. 6 requires a special coupling procedure, this difficulty can be overcome in a similar manner as the procedure outlined in the RFMB derivation. Combining the rigid-body modes with the redundant boundary constraint modes into a single constraint mode set, the HMB coordinate transformation is expressed as

$$\begin{Bmatrix} x_b \\ x_c \\ x_i \end{Bmatrix} = \begin{bmatrix} \backslash I_b \backslash & 0 & 0 & 0 \\ 0 & \backslash I_c \backslash & 0 & 0 \\ \psi_{\mathrm{ib}}^C & \psi_{\mathrm{ic}}^C & \psi_{\mathrm{ir}}^I & \phi_{\mathrm{ik}}^N - \psi_{\mathrm{ic}}^C \phi_{\mathrm{ck}}^N \end{bmatrix} \begin{Bmatrix} x_b \\ x_c \\ q_r \\ q_k \end{Bmatrix} \tag{16}$$

where ψ_r^I is the inertia-relief mode set composed of r columns corresponding to the number of component rigid-body modes. For the all-fixed-boundary case, Hintz's paper compares the convergence of the HMB vs the Hurty/Craig–Bampton method for the Benfield-truss problem (Fig. 1). For the same number of retained DOF in the combined truss model (12, 20, 28 DOF out of a 60 DOF combined physical model), HMB gives superior convergence for the lower frequencies, whereas Hurty/Craig–Bampton gives superior convergence for the higher frequencies. For example, for the 12-DOF truss problem, the HMB percent frequency error is 0.00069% for the fundamental mode to 0.0112% for Hurty/Craig–Bampton. However, for the fifth mode HMB results in 10.3% error compared to 0.19% for Hurty/Craig–Bampton. This is not surprising given the presence of low-frequency inertia-relief modes in HMB, which should improve the convergence for the lower-frequency system modes, while the additional high-frequency normal modes content of Hurty/Craig–Bampton should improve the convergence of higher-frequency system modes. For the all-free-boundary case, the convergence of HMB is expected to be similar to Rubin's method [Eq. (9)], that is, from a vector space equivalence perspective the method is equivalent to Rubin's for the all-free-boundary case. The presence of inertia-relief modes can increase the potential for rank deficiency, as will be addressed in Sec. V. Most importantly, the HMB generalized stiffness matrix contains parameters that cannot be directly derived from component testing.

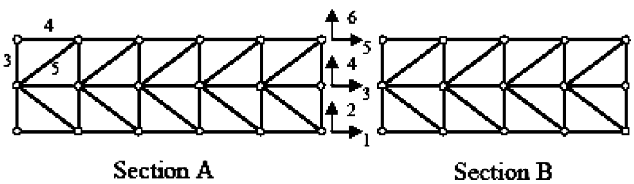

Fig. 1 Benfield-truss problem.

The MHMB method is a popular variation of HMB, where the inertia-relief modes are not employed, resulting in

$$\begin{Bmatrix} x_b \\ x_c \\ x_i \end{Bmatrix} = \begin{bmatrix} \backslash I_b \backslash & 0 & 0 \\ 0 & \backslash I_c \backslash & 0 \\ \psi_{\mathrm{ib}}^C & \psi_{\mathrm{ic}}^C & \phi_{\mathrm{ik}}^N - \psi_{\mathrm{ic}}^C \phi_{\mathrm{ck}}^N \end{bmatrix} \begin{Bmatrix} x_b \\ x_c \\ q_k \end{Bmatrix} \tag{17}$$

Because the combination of constraint modes and normal modes (with the $\bar{B}$ set constrained) span the same space as residual flexibility and normal modes, MHMB and RFMB are equivalent for the all-fixed-boundary and mixed-boundary cases. However, this equivalence does not hold for the all-free-boundary case, resulting in slow convergence and appreciable frequency errors for MHMB as will be demonstrated in the Benfield-truss example problem. This slow convergence for the all-free-boundary case is a direct result of the elimination of inertia-relief modes in MHMB.

Because the MHMB generalized stiffness matrix will be utilized for comparison to RFMB generalized stiffness in Sec. IV, the MHMB generalized stiffness (and mass) will be derived here. The MHMB generalized stiffness matrix (in the q_1 space) is given by

$$\kappa_1^{\mathrm{MHMB}} = \begin{bmatrix} \kappa_{\mathrm{bb}} & \kappa_{\mathrm{bc}} & 0 \\ \kappa_{\mathrm{cb}} & \kappa_{\mathrm{cc}} & \kappa_{\mathrm{ck}} \\ 0 & \kappa_{\mathrm{kc}} & \backslash \omega_k^2 \backslash \end{bmatrix} \tag{18}$$

where the free boundary to normal modes coupling terms are given by

$$\kappa_{\mathrm{ck}} = \kappa_{\mathrm{kc}}' = \psi_c^{C'} k \phi_k^N \tag{19}$$

The generalized mass matrix is similarly derived, resulting in a fully populated matrix:

$$\mu_1^{\mathrm{MHMB}} = \begin{bmatrix} \mu_{\mathrm{bb}} & \mu_{\mathrm{bc}} & \mu_{\mathrm{bk}} \\ \mu_{\mathrm{cb}} & \mu_{\mathrm{cc}} & \mu_{\mathrm{ck}} \\ \mu_{\mathrm{kb}} & \mu_{\mathrm{kc}} & \backslash I_k \backslash \end{bmatrix} \tag{20}$$

The RFMB-V (V for variant) method was developed by Majed[9] as an extension of Bamford's method[10] to mixed boundary. The variant uses total flexibility for the $\bar{C}$ set coupling terms. Given that residual flexibility and normal modes combination spans the same subspace as total flexibility and normal modes, this variation is equivalent to RFMB for all boundary conditions. The derivation follows along the same lines as the RFMB method. The resulting coordinate transformation is given by

$$\begin{Bmatrix} x_b \\ x_c \\ x_i \end{Bmatrix} = \begin{bmatrix} \backslash I_b \backslash & 0 & 0 \\ 0 & \backslash I_c \backslash & 0 \\ \psi_{\mathrm{ib}}^C - g_{\mathrm{ic}}^T g_{\mathrm{cc}}^{T^{-1}} \psi_{\mathrm{cb}}^C & g_{\mathrm{ic}}^T g_{\mathrm{cc}}^{T^{-1}} & \phi_{\mathrm{ik}}^N - g_{\mathrm{ic}}^T g_{\mathrm{cc}}^{T^{-1}} \phi_{\mathrm{ck}}^N \end{bmatrix} \begin{Bmatrix} x_b \\ x_c \\ q_k \end{Bmatrix} \tag{21}$$

In contrast to the RFMB, the RFMB-V generalized stiffness parameters cannot be directly derived from test.

IV. Test/Analysis Correlation

In his paper,[5] Rubin emphasized the key aspect of his free-boundary method, that is, the ability to directly validate the parameters of the method's generalized stiffness from a component free-modal test data. The ability to validate such parameters directly from test leads to a more rigorous test/analysis correlation, going well beyond the standard correlation practice of frequencies and normal modes. The RFMB method generalized stiffness matrix parameters can also be directly validated from component testing; it will be shown later in this section that this is not true for any other mixed-boundary method. Of course, it is not surprising that the key element common in both methods is residual flexibility.

Martinez and Gregory[11] conclude that methods involving residual flexibility are best suited for direct determination of component parameters from test. Time-tested, practical techniques by Rubin,[5] Lamontia,[12] and Klosterman[13] are readily available for determining residual flexibility directly from component modal test data and will be briefly discussed in the following paragraph.

Consider the RFMB generalized stiffness matrix given in Eq. (10) and restated here:

$$\kappa_1^{\text{RFMB}} = T_1' k T_1 = \begin{bmatrix} \kappa_{\text{bb}} & & \\ & g_{\text{cc}}^R & \\ & & \backslash\omega_{k\backslash}^2 \end{bmatrix} \tag{10}$$

The block-diagonal form (i.e., no cross-coupling terms) of the RFMB generalized stiffness along with the explicit presence of the $\bar{C}$ set residual flexibility g_{cc}^R are the key features that allow test/analysis correlation of all parameters in the RFMB generalized stiffness. The component $\bar{B}$ set stiffness κ_{bb}, which is constrained in the modal test, can be determined from a static (influence coefficient) test. Relative to the modal test, the only additional requirement imposed is the determination of the $\bar{C}$ set residual flexibility g_{cc}^R. Rubin[5] outlines an approach for deriving the residual data (i.e., residual flexibility along with the second-order residual damping and residual mass) from component modal test data. The approach involves the experimental determination of the dynamic flexibility matrix for the $\bar{C}$ set DOF via application of the exciter force at one $\bar{C}$ set DOF at a time and recording the response displacements at all other $\bar{C}$ set DOF under the steady-state sinusoidal conditions. Subtracting the retained modal data from the dynamic flexibility matrix then yields the residual dynamic flexibility matrix. What remains is to approximate the residual dynamic flexibility matrix over the frequency range of interest by the second-order form of the displacement equation involving residual flexibility, damping, and mass given by [Eqs. (23) and (49) in Ref. 5]:

$$x_c^R(\omega) = g_{\text{cc}}^R + \varpi^2 \mu_{\text{cc}}^R - i\varpi c_{\text{cc}}^R \tag{22}$$

Rubin states that if this second-order form provides a good fit to the residual dynamic flexibility matrix the goal is achieved. He further states that a poor curve fit might be caused by: "a) measurement errors in the (retained) modal parameters, b) the need to experimentally determine additional modes, or c) departures from the assumptions of linearity and classical modal damping." He goes on to say that the practicality of this approach has been demonstrated relative to residual flexibility with the conclusion that "the approach is extremely attractive since it is practically feasible for large complex systems. . . ." Lamontia[12] and Klosterman[13] further discuss the experimental determination of the residual flexibility matrix.

In contrast, the MHMB generalized stiffness matrix (along with other mixed-boundary variants), restated next, involves various cross-coupling terms, which present difficulties for direct determination from test. It is not immediately apparent to the authors how the cross-coupling terms $\kappa_{\text{ck}} = \kappa_{\text{kc}}' = \psi_c^{C'} k \phi_k^N$, which represent the coupling between free-boundary and normal modes, can be determined from test:

$$\kappa_1^{\text{MHMB}} = \begin{bmatrix} \kappa_{\text{bb}} & \kappa_{\text{bc}} & 0 \\ \kappa_{\text{cb}} & \kappa_{\text{cc}} & \kappa_{\text{ck}} \\ 0 & \kappa_{\text{kc}} & \backslash\omega_{k\backslash}^2 \end{bmatrix} \tag{18}$$

V. Some Words on the Rank of Mixed-Boundary Methods

The rank of the mixed-boundary methods can be best studied by assuming an untruncated normal mode set. Because practical application of component reduction methods often involves a significant level of normal mode truncation, this section might be of only an academic value.

For the HMB method, an untruncated normal mode set will implicitly contain both the $\bar{C}$ set constraint modes as well as the inertia-relief modes resulting in up to $c + r$ singularities for the mixed-boundary and all-free-boundary cases. For the all-fixed-boundary case, HMB can result up to r singularities for an untruncated normal mode set.

It was demonstrated in Sec. III that the MHMB, RFMB, and RFMB-V methods are equivalent for the all-fixed- and mixed-boundary cases. For an untruncated normal mode set, these methods result in up to c singularities for the mixed-boundary case and zero singularities for the all-fixed-boundary case. For the all-free-boundary case, each of these methods can result in up to c singularities for an untruncated normal mode set.

Certain special cases can result in a rank deficiency of a similar nature as that of employing an untruncated normal mode set. These special cases might very well fit into the category of user misapplication of mixed-boundary methods, pushing the methods beyond their mathematical limitations. For instance, consider a case where mechanism DOF are placed in the $\bar{C}$ set. These mechanism rigid-body modes will be implicitly contained in the constraint modes, resulting in linear dependencies with the mechanism rigid-body normal modes in both HMB as well as MHMB. Similarly, but via a different mathematical route, these mechanism DOF result in rank deficiencies in the RFMB and RFMB-V methods because the mechanism rigid-body modes will contain the total flexibility for the DOF, leaving zero residual flexibility.

For a second special case, consider a case where seismic masses are placed on the $\bar{C}$ set. It is assumed that the user's intent is to base-drive the component, in which case the placement of the base-drive DOF in the $\bar{B}$ set would result in the desired cantilevered modes; nevertheless, we will address this special case. The seismic masses will force the $\bar{C}$ set DOF to become node points in the normal modes, resulting in both zero total and zero residual flexibility for the subject DOF. This results in up to c singularities in the RFMB and RFMB-V methods. From a methods equivalence argument, it is clear that the seismic masses will also result in the same order singularity in the HMB and MHMB methods.

A simple solution to these "user misapplications" is for the user to place mechanism and seismic mass DOF in the $\bar{B}$ set instead. A second simple work-around would be to couple in the mechanism and seismic mass DOF to the $\bar{C}$ set after the reduction.

With the practical use of component reduction methods most often involving significant levels of normal mode truncation, the issue of rank deficiency is academic. However, it is a simple exercise to prove that the rank of the RFMB coordinate transformation in Eq. (7) is $b + c + k$, that is, fully ranked for a truncated set of normal modes. To show this, the following two theorems from Ref. 14 are utilized:

1) Theorem 9: If $B = PAQ$, where P and Q are nonsingular matrices, then A and B are equivalent.

2) Theorem 11: Two $(m \times n)$ matrices are equivalent if and only if they have the same rank.

We will begin with the coordinate transformation matrix T_1 in Eq. (3). The coordinate transformation is composed of 1) constraint modes for the fixed boundary, 2) residual flexibility for the free boundary (relative to the fixed boundary), and 3) a truncated set of normal modes (relative to the fixed boundary). It is clear that these mode sets are by definition mutually linearly independent resulting in a rank of $b + c + k$.

Per Theorem 9, the matrix multiplication in Eq. (6) will result in the RFMB transformation being of the same rank as T_1 (equivalent matrices having the same rank per Theorem 11) if the T_2 matrix is nonsingular. In other words, the T_2 matrix is substituted as the Q matrix in Theorem 9, the A matrix being T_1 and the P matrix being identity. It is easily demonstrated that the T_2 matrix is nonsingular,

Table 2 Percent frequency error for all-fixed and all-free boundaries[a]

Elastic mode number	Craig–Bampton fixed-boundary normal modes[b]	Rubin free-boundary normal modes[c]	MHMB all-fixed-boundary normal modes[b]	MHMB all-free-boundary normal modes	RFMB all-fixed-boundary normal modes[b]	RFMB all-free-boundary normal modes[c]
1	0.00	0.00	0.00	0.00	0.00	0.00
2	0.00	0.00	0.00	0.00	0.00	0.00
3	0.02	0.01	0.02	9.25	0.02	0.01
4	0.01	0.00	0.01	0.00	0.01	0.00
5	0.01	0.00	0.01	0.00	0.01	0.00
6	0.01	0.01	0.01	0.01	0.01	0.01
7	1.22	0.03	1.22	0.80	1.22	0.03
8	0.09	0.03	0.09	0.02	0.09	0.03
9	0.28	0.07	0.28	0.07	0.28	0.07
10	0.10	0.46	0.10	0.42	0.10	0.46
11	0.18	0.04	0.18	0.03	0.18	0.04
12	0.08	1.69	0.08	1.53	0.08	1.69
13	0.31	1.58	0.31	5.23	0.31	1.58
14	0.69	1.72	0.69	4.29	0.69	1.72
15	7.06	11.00	7.06	13.60	7.06	11.00
16	2.03	8.62	2.03	28.66	2.03	8.62
17	4.12	20.37	4.12	39.83	4.12	20.37
18	14.63	21.61	14.63	41.55	14.63	21.61
19	17.04	31.23	17.04	53.41	17.04	31.23
20	32.05	36.59	32.05	46.22	32.05	36.59
21	93.51	94.04	93.51	94.09	93.51	94.04

[a]Section A has 11 normal modes, and section B has 7 normal modes. [b]Identical columns. [c]Identical columns.

that is,

$$T_2^{-1} = \begin{bmatrix} I & 0 & 0 \\ -g_{\text{cc}}^{R^{-1}}\psi_{\text{cb}}^{C} & -g_{\text{cc}}^{R^{-1}} & -g_{\text{cc}}^{R^{-1}}\phi_{\text{ck}}^{N} \\ 0 & 0 & I \end{bmatrix}^{-1}$$

$$= \begin{bmatrix} I & 0 & 0 \\ -\psi_{\text{cb}}^{C} & -g_{\text{cc}}^{R} & -\phi_{\text{ck}}^{N} \\ 0 & 0 & I \end{bmatrix} \tag{23}$$

Therefore, from Theorems 9 and 11 the rank of the resulting RFMB transformation matrix is the same as T_1, that is, $b + c + k$.

VI. Example Problems

A. Benfield-Truss Problem

The two-dimensional, two-section Benfield truss, illustrated in Fig. 1, has historically been used to test CMS methodology convergence (see Ref. 7). As illustrated, section A consists of five identical bays with section B consisting of four. The coupled system consists of 60 DOF. The vertical members, horizontal members, and diagonal members have length ratios of 3, 4, and 5, respectively, with equal cross-sectional areas.

For this part of the exercise, the two mixed-boundary methods will use identical sets of normal modes as used in Hurty/Craig–Bampton and Rubin's methods to ensure a consistent comparison basis. The results are presented as percent differences from the "exact" solution, derived from the complete 60-DOF eigensolution. Note that convergence for all methods falters after the 14th predicted elastic mode.

The results are presented in Table 2. It is clear that the RFMB method is exactly equal to the Hurty/Craig–Bampton and Rubin for the all-fixed- and all-free-boundary cases, as expected from Eqs. (8) and (9). In contrast, although the MHMB method is exactly equal to Hurty/Craig–Bampton for the all-fixed case, it results in frequency errors as high as 9.2% in the third mode of the Benfield-truss problem.

B. Space Shuttle Cargo Carrier

The second example problem involves a 650,000+ DOF finite element math model of a shuttle cargo carrier, depicted in Fig. 2.

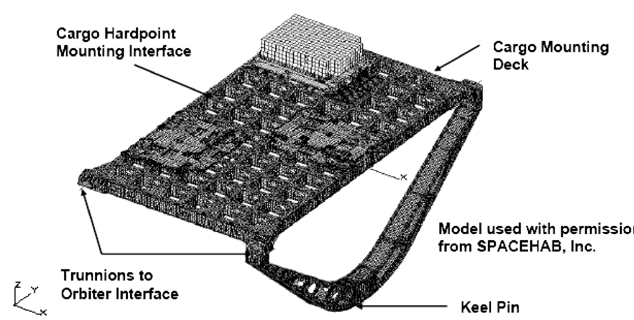

Fig. 2 High-fidelity finite element model of a space shuttle cargo carrier.

The cargo carrier attaches to the shuttle via trunnions and keel pin with a total of 8 DOF. The cargo carrier provides 41 DOF for cargo attach. The cargo carrier finite element model is to be reduced and then coupled with various cargo reduced models via the 41-DOF boundary in a CMS process. The space shuttle program requirement for the integrated cargo carrier + cargos reduced math model is to have accuracy up to 75 Hz relative to the orbiter attach DOF (the eight boundary DOF). To achieve this requirement, it is prudent for the cargo carrier reduced math model representation to be accurate up to 150 Hz relative to the same orbiter attach dofs.

The RFMB employs normal modes with the orbiter attach DOF fixed ($\bar{B}$ set). The cargo attach dofs ($\bar{C}$ set) are added via residual flexibility as shown in the derivation of the coordinate transformation. The results of an eigenvalue problem conducted on the resulting RFMB stiffness and mass matrices, Eqs. (13) and (14) are given in Table 3. As expected, there is zero-frequency error vs the full model eigenvalue problem.

The subsequent columns in Table 3 exhibit the convergence of the overconstrained Hurty/Craig–Bampton method, that is, normal modes relative to the combined $\bar{B}$ and $\bar{C}$ set dofs being fixed. The table illustrates that in order to achieve a "clean" convergence (<1%), a linear combination of over 242 overconstrained normal modes (up to 400 Hz) is required. This 291-DOF overconstrained Hurty/Craig–Bampton reduction took 4 h and 56 min on a high-speed workstation, whereas the 73-DOF RFMB reduction was executed in just 59 min on the same platform.

Table 3 Percent frequency error: RFMB vs Hurty/Craig–Bampton

Mode no.	Exact frequency, Hz	RFMB ——	Guyan ——	Guyan +8 modes (100 Hz)	Guyan +15 modes (150 Hz)	Guyan +24 modes (200 Hz)	Guyan +42 modes (250 Hz)	Guyan +74 modes (300 Hz)	Guyan +242 modes (400 Hz)
1	18.06	0.00	0.79	0.53	0.33	0.02	0.01	0.01	0.00
2	21.29	0.00	2.94	0.15	0.07	0.04	0.03	0.02	0.00
3	30.07	0.00	2.53	1.39	0.42	0.09	0.04	0.03	0.01
4	32.87	0.00	5.16	1.23	0.46	0.08	0.06	0.05	0.00
5	47.77	0.00	32.52	0.37	0.11	0.04	0.02	0.01	0.01
6	50.40	0.00	34.70	0.42	0.14	0.04	0.03	0.02	0.00
7	53.70	0.00	71.87	1.16	0.33	0.14	0.09	0.05	0.02
8	59.67	0.00	69.60	1.37	0.36	0.22	0.11	0.06	0.02
9	67.25	0.00	74.04	3.01	1.00	0.23	0.13	0.06	0.04
10	82.43	0.00	48.09	4.70	1.42	0.97	0.55	0.34	0.12
11	84.01	0.00	53.48	7.78	0.71	0.24	0.17	0.11	0.05
12	86.65	0.00	52.11	6.08	2.05	1.31	0.78	0.53	0.17
13	90.93	0.00	63.60	9.44	3.02	0.74	0.33	0.21	0.12
14	92.91	0.00	——	13.26	1.77	0.53	0.36	0.19	0.08
15	101.94	0.00	——	16.91	3.13	2.86	2.75	1.56	0.23
16	105.69	0.00	——	18.69	1.64	1.21	0.99	0.17	0.03
17	108.07	0.00	——	19.83	4.65	3.36	2.82	0.76	0.21
18	113.95	0.00	——	19.27	7.57	3.82	3.35	1.89	0.29
19	119.36	0.00	——	——	7.72	4.87	2.28	1.41	0.44
20	130.08	0.00	——	——	1.26	0.68	0.42	0.21	0.09
21	131.51	0.00	——	——	7.96	0.86	0.51	0.33	0.15
22	139.00	0.00	——	——	——	2.94	1.64	0.90	0.41
23	141.07	0.00	——	——	——	2.99	1.26	0.78	0.39
24	147.62	0.00	——	——	——	——	——	1.58	0.76

VII. Conclusions

A residual flexibility mixed-boundary (RFMB) method of component representation is presented. The RFMB method involves three mutually linearly independent mode sets: the constraint modes representing the fixed boundary, residual flexibility representing the free boundary, and a truncated set of normal modes relative to the fixed-boundary. It was demonstrated that RFMB is accurate through the entire range of component boundary degrees-of-freedom representation, from all-fixed to mixed, to all-free boundaries. It was shown that this is not the case for the popular modified-Hintz mixed-boundary (MHMB) method, which degenerates for the all-free-boundary case resulting in appreciable frequency errors as demonstrated in the classical Benfield-truss example problem.

Furthermore, it was shown that the RFMB generalized stiffness matrix, which involves no cross-coupling terms, is the most likely candidate for direct determination/validation from component testing, in a manner analogous to Rubin's generalized stiffness from free component modal testing. Mixed-boundary variants such as MHMB involve terms coupling the free boundary to the normal modes, which cannot be directly determined from component testing.

The RFMB accuracy for all possible mix of component boundary representations along with the ability to directly determine/validate the RFMB generalized stiffness from test present two compelling features of the method to be considered by the technical community.

References

[1]Craig, R. R., Jr., "Coupling of Substructures for Dynamic Analyses: An Overview," AIAA Paper 2000-1573, April 2000.

[2]Hurty, W. C., "Dynamic Analysis of Structural Systems Using Component Modes," *AIAA Journal*, Vol. 3, No. 4, 1965, pp. 678–685.

[3]Craig, R. R., Jr., and Bampton, M. C. C., "Coupling of Structures for Dynamic Analyses," *AIAA Journal*, Vol. 6, No. 7, 1968, pp. 1313–1319.

[4]MacNeal, R. H., "A Hybrid Method of Component Mode Synthesis," *Journal of Computers and Structures*, Vol. 1, No. 4, 1971, pp. 581–601.

[5]Rubin, S., "An Improved Component-Mode Representation," *AIAA Journal*, Vol. 13, No. 8, 1975, pp. 995–1006.

[6]Benfield, W. A., and Hruda, R. F., "Vibration Analysis of Structures by Component Mode Substitution," *AIAA Journal*, Vol. 9, No. 7, 1971, pp. 1255–1261.

[7]Hintz, R. M., "Analytical Methods in Component Modal Synthesis," *AIAA Journal*, Vol. 13, No. 8, 1975, pp. 1007–1016.

[8]Collins, J. D., Hart, G. C., Hurty, W. C., and Kennedy, B., "Review and Development of Modal Synthesis Techniques," J. H. Wiggins Co., TR 1073-1, Redondo Beach, CA, 1972.

[9]Majed, A., "An Improvement to Bamford's Modal Synthesis," Notes for CMS Technical Briefing, Rockwell International, Downey, CA, June 1989.

[10]Bamford, R., Wada, B. K., Garba, J. A., and Chisholm, J., "Dynamic Analysis of Large Structural Systems," *Synthesis of Vibrating Systems*, American Society of Mechanical Engineers, 1971, pp. 57–71.

[11]Martinez, D. M., and Gregory, D. L., "A Comparison of Free Component Mode Synthesis Techniques Using MSC/NASTRAN," Sandia National Lab., Rept. SAND83-0025, Albuquerque, NM, June 1984.

[12]Lamontia, M. A., "On the Determination and Use of Residual Flexibilities, Inertia Restraints, and Rigid-Body Modes," *Proceedings of the 1st International Modal Analysis Conference*, Union College, Schenectady, NY, 1982, pp. 153–159.

[13]Klosterman, A. L., "On the Experimental Determination and Use of Modal Representations of Dynamic Characteristics," Ph.D. Dissertation, Dept. of Mechanical Engineering, Univ. of Cincinnati, Cincinnati, OH, 1971.

[14]Wyle, C. R., "Determinants and Matrices," *Advanced Engineering Mathematics*, 3rd ed., McGraw–Hill, New York, 1960, Chap. 10.

L. Peterson
Associate Editor